Making sense of all that AVO stuff!

Brian Russell
Hampson-Russell, A CGGVeritas Company
Suite 510, 715 5th Ave. SW, Calgary, Alberta, Canada, T2P 2X6
brian.russell@cggveritas.com

SUMMARY

The Amplitude Variations with Offset (AVO) technique, and the related technique of pre-stack seismic inversion, has grown to include a multitude of sub-techniques, each with its own assumptions. This vast array of techniques makes it difficult for the interpreting geophysicist to understand how they are all related, and which method should be used in a particular exploration area. In this talk I will present a framework from which all of the current AVO and pre-stack seismic inversion methods can be understood. This will involve looking at the concept of seismic reflectivity in its various forms, as well as inverted reflectivity, or impedance. To illustrate the various AVO and pre-stack inversion techniques, I will use a gas sand example from central Alberta, Canada.

Key words: AVO, pre-stack seismic inversion, acoustic impedance, shear impedance, elastic impedance.

INTRODUCTION

For a layered earth, a well log measures a parameter *P* for each layer and the seismic trace measures the interface reflectivity *R* convolved with the seismic wavelet. The measured parameter and its associated reflectivity for a typical earth model is shown schematically in Figure 1.

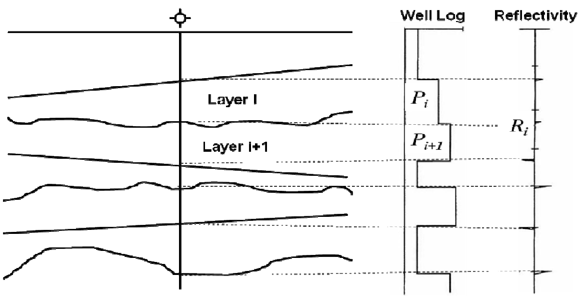

Figure 1: A schematic illustration of well log and seismic mesurements, where a well log measures a parameter *P* for each layer in the earth (left and center panels) and the seismic data records the reflectivity (*R*) at each interface.

Despite the apparent complexity of current Amplitude Variations with Offset (AVO) methodology, Figure 1 serves as a good starting point for understanding all of the various AVO methods. That is, AVO techniques can be subdivided into two broad categories: (1) seismic reflectivity methods and (2) impedance methods, where impedance is a type of parameter that can be measured by the well log. We will start with a discussion of seismic reflectivity methods.

SEISMIC REFLECTIVITY METHODS

The linearlized reflectivity at each interface can be found by dividing the change in the value of the parameter by twice its average, or

$$R_i = \frac{P_{i+1} - P_i}{P_{i+1} + P_i} = \frac{\Delta P_i}{2\overline{P}_i}, \tag{1}$$

where $\Delta P_i = P_{i+1} - P_i$ and $\overline{P}_i = \dfrac{P_{i+1} + P_i}{2}$.

But which parameter *P* are we interested in? To the geophysicist the choices usually are: *P*-wave velocity (V_P), *S*-wave velocity (V_S), and density (ρ), or transforms of velocity and density such as acoustic impedance (*AI*, which is defined as ρV_P) and shear impedance (*SI*, which is defined as ρV_S). The geologist would add parameters like gamma ray, water saturation, porosity and other geological parameters. How many of these can we derive from the seismic data?

Let us start by looking at a seismic example. Figure 2 shows the stack over a gas sand from Alberta, where the gas "bright spot" is shown in the centre of the line at at time of 640 ms.

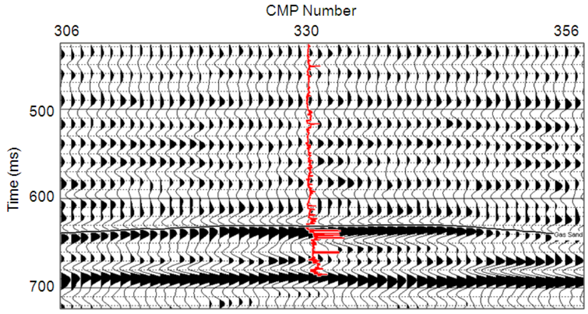

Figure 2: A portion of a stacked seismic section over a gas sand in Alberta.

Our assumption is that the stacked section represents a seismic wavelet convolved with the reflectivity derived from changes in the acoustic impedance, in which case equation 1 can be re-written as

$$R_{AI} = R_{VP} + R_D = \frac{\Delta AI}{2AI}, \tag{2}$$

where $R_{VP} = \dfrac{\Delta V_P}{2\overline{V}_P}$ and $R_D = \dfrac{\Delta\rho}{2\overline{\rho}}$.

Notice that three different reflectivities have been defined in equation 2, the acoustic impedance reflectivity, which is in turn the sum of the P-wave velocity reflectivity and the density reflectivity. The only missing term is the shear-wave reflectivity. Measuring the shear-wave effects are crucial in seismic exploration since if we compare the shear and compressional terms we can estimate fluid properties. Equation 2 is the equation for reflectivity at an angle of zero degrees, and makes it clear that traditional stacked seismic data is ambiguous when it comes to detecting fluid anomalies. Thus, even though we suspect that the "bright spot" on the stack in Figure 2 is due to gas, we can't be sure.

Ostrander (1984) suggested that with pre-stack seismic data, we we should be able to detect shear-wave effects. Figure 3 shows the corrected pre-stack gathers over central portion of the same gas sand shown in Figure 2. It is clear that there is an amplitude increase with offset (and therefore angle) at the gas sand zone at 640 ms.

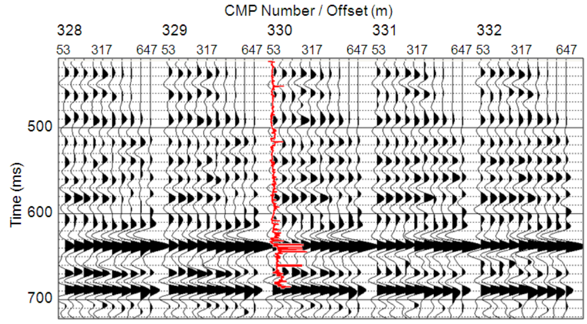

Figure 3: The CDP gathers over a portion of the stack in Figure 2.

To understand how to quantify this amplitude increase with offset we start with the work of Aki and Richards (2002), who extended the reflectivity in equation 2 to angles greater than zero using a linearized version of the Zoeppritz equations, which is written:

$$R(\theta) = aR_{VP} + bR_{VS} + cR_D, \qquad (3)$$

where $a = 1 + \tan^2\theta$, $b = -8\left(\frac{\bar{V}_S}{\bar{V}_P}\right)^2 \sin^2\theta$,

$c = 1 - 4\left(\frac{\bar{V}_S}{\bar{V}_P}\right)^2 \sin^2\theta$, and $R_{VS} = \frac{\Delta V_S}{2\bar{V}_S}$.

Notice that the shear wave reflectivity term, R_{VS}, appears explicitly in this equation, and thus can be extracted using a least-squares inversion scheme. In fact, the Aki-Richards equation of equation 3 is the basis of virtually all AVO methods.

The most common reflectivity analysis method is a re-formulation of equation 3 that was given by Wiggins et al. (1983) and is written

$$R(\theta) = R_{AI} + G\sin^2\theta + R_{VP}\sin^2\theta\tan^2\theta, \qquad (4)$$

where $G = R_{VP} - 8(\bar{V}_S/\bar{V}_P)^2 R_{VS} - 4(\bar{V}_S/\bar{V}_P)^2 R_D$ is the gradient and $R_{VS} = \frac{\Delta V_S}{2\bar{V}_S}$. By transforming the CDP gathers in Figure 3 from offset to angle, and picking the amplitudes as a function of angle, we are able to perform at least-squares fit at each time and CDP to extract the R_{AI} and G terms in equation 4. The acoustic impedance reflectivity is often called the intercept term, since on a plot of amplitude versus angle it intercepts the amplitude axis at an angle of zero degrees.

Figure 4 shows a cross-plot of intercept versus offset around the gas sand zone of Figure 3, where the top-of-gas zone (pink), base-of-gas zone (yellow) and sub-gas carbonate stringers (blue) have all been highlighted. This is referred to as a class 3 AVO anomaly (Rutherford and Williams, 1989), since the top-of- gas event shows and a large negative intercept and gradient and the base-of-gas event shows a large positive intercept and gradient.

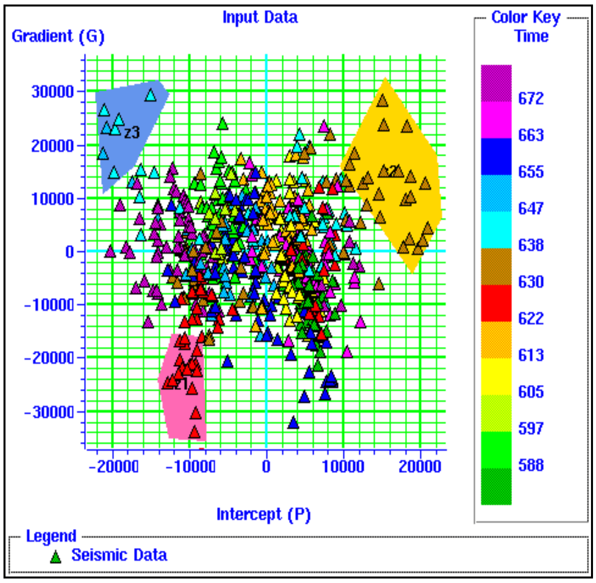

Figure 4: A cross-plot of the intercept and gradient terms from equation (4), extracted around the gas sand zone of the data in Figure 3, where the top-of-gas zone is in pink, the base-of-gas zone is in yellow and the sub-gas carbonate stringers are in blue.

Figure 5 then shows the respective zones from the cross-plot superimposed on the original stacked seismic section. Notice the excellent delineation of the gas sand.

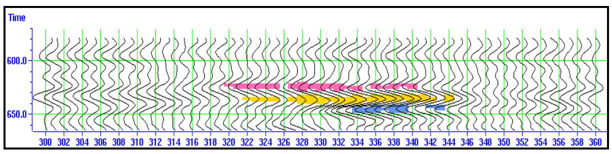

Figure 5: The position of the cross-plot zones on the seismic stack of Figure 2, (top-of-gas zone = pink, base-of-gas zone = yellow and sub-gas carbonate stringers = blue.)

Although the intercept-gradient cross-plot technique is the most popular reflectivity methods, there are also several other methods, such as near and far trace stacking and the fluid factor method (Smith and Gidlow, 1987). Near and far trace stacks (from which we can take differences) are the simplest AVO attributes to interpret, but lack a physical model. This model can be supplied by inverting these stacks to produce elastic impedance. Also, the fluid factor method can be extended by inverting to Poisson impedance. Impedance methods will be summarized next.

SEISMIC IMPEDANCE METHODS

The second set of AVO methods, called impedance methods and are based on the inversion of the reflectivity estimates to give impedance. This can be done using a second re-reformulation of the Aki-Richards equation that was given by Fatti et al. (1994) as:

$$R(\theta) = aR_{AI} + bR_{SI} + c' R_D, \qquad (5)$$

where:

$$R_{SI} = \frac{\Delta SI}{2SI} = R_{VS} + R_D,$$

and $c' = 4(\overline{V}_S / \overline{V}_P)^2 \sin^2\theta - \tan^2\theta$.

We can use equation 5 to extract and invert the reflectivity terms to acoustic and shear impedance, and possibly density (Hampson et al., 2005). That is:

$$R_{AI} \Rightarrow AI = \rho V_P \text{ (Acoustic Impedance)}$$
$$R_{SI} \Rightarrow SI = \rho V_S \text{ (Shear Impedance)}$$
$$R_D \Rightarrow \rho \text{ (Density)}$$

A useful physical parameter that can be derived from the acoustic and shear impedance is the V_P/V_S ratio, since the density term will cancel in the division. Once the inversion has been done, a cross-plot can again be used to delineate the gas sand. Figure 6 shows a cross-plot of inverted acoustic impedance (horizontal axis) versus V_P/V_S ratio (vertical axis) for the gas sand zone of the stack in Figure 2, with the gas sand points highlighted in red.

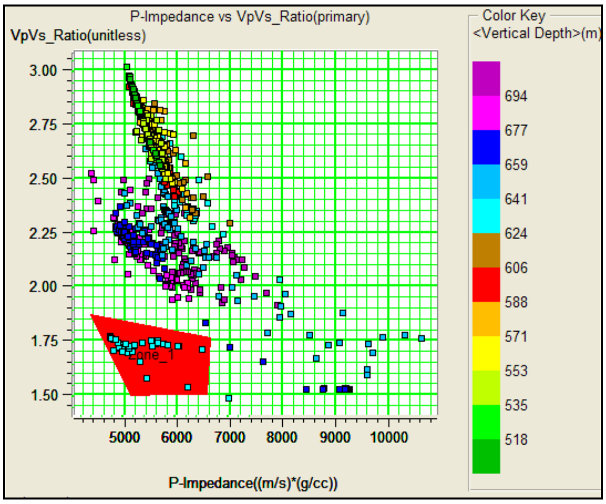

Figure 6: A cross-plot of the inverted acoustic impedance and V_P/V_S ratio terms extracted from around the gas sand zone of the data in Figure 2, where the gas zone is in red.

Figure 7 then shows the respective zones from the cross-plot of Figure 6 superimposed on the original stacked seismic section. Again, notice the excellent delineation of the gas sand.

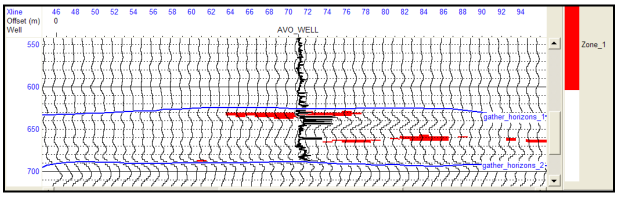

Figure 7: The position of the cross-plot zones on the seismic stack of Figure 2, (gas zone = red).

There are also numerous other impedance methods used in AVO, such as the elastic impedance (EI) and extended elastic impedance (EEI) methods (Connolly, 1999, Whitcombe et al., 2002), the lambda-mu-rho, or LMR, method (Goodway et al., 1997) and the Poisson Impedance, or PI, method (Quakenbush et al., 2006). As mentioned in the last section, elastic impedance can be thought of as an impedance extension of near and far trace stacking, and Poisson impedance as an extension of the fluid factor method. Finally, the LMR method extends the acoustic and shear impedance inversion method just discussed by transforming to more basic elastic parameters. For all of these methods, their results can be best interpreted using cross-plot analysis.

CONCLUSIONS

In this tutorial we have shown how Amplitude Variations with Offset, or AVO, techniques can be subdivided into two broad categories: (1) seismic reflectivity methods and (2) impedance methods. Seismic reflectivity methods include: Near and Far stacks, Intercept vs Gradient analysis and the fluid factor. Impedance methods, which are often referred to as pre-stack seismic inversion methods include: P and S-impedance inversion, Lambda-mu-rho, Elastic Impedance and Poisson Impedance. These subdivisions are shown in Figure 8.

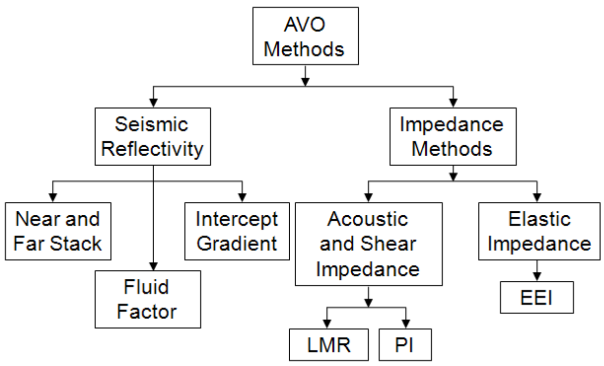

Figure 8: A classification scheme for AVO and pre-stack seismic inversion methods.

Several of these methods were applied to a prospective gas sand anomaly on a dataset from central Alberta, and we found that we were able to delineate the gas sand extremely well using these techniques.

The AVO technique used in a particular area will depend on both the software available to the geoscientist and the quality of the seismic data. In general, there is no one method that will give optimum results everywhere. Optimization of parameters and an understanding of the exploration objective are crucial to the success of any AVO method.

ACKNOWLEDGMENTS

I wish to thank my colleagues Dan Hampson and Graham Carter for their many suggestions that improved this tutorial.

REFERENCES

Aki, K., and Richards, P.G., 2002, Quantitative Seismology, 2nd Edition: W.H. Freeman and Company.

Connolly, P., 1999, Elastic impedance: The Leading Edge, 18, no. 4, 438-452.

Fatti, J., Smith, G., Vail, P., Strauss, P., and Levitt, P., 1994, Detection of gas in sandstone reservoirs using AVO analysis: a 3D Seismic Case History Using the Geostack Technique: Geophysics, 59, 1362-1376.

Goodway, W., Chen, T., and Downton, J., 1997, Improved AVO fluid detection and lithology discrimination using Lamé petrophysical parameters: Extended Abstracts, SEG 67th Annual International Meeting, Denver.

Hampson, D., Russell, B. and Bankhead, B., 2005, Simultaneous inversion of pre-stack seismic data: SEG, Expanded Abstracts, 24, no. 1, 1633-1637.

Ostrander, W. J., 1984, Plane-wave reflection coefficients for gas sands at non-normal angles of incidence: Geophysics, 49, 1637-1648.

Quakenbush, M., Shang, B., and Tuttle, C., 2006, Poisson impedance: The Leading Edge, 25, no. 2, 128-138.

Rutherford, S. R. and Williams, R. H., 1989, Amplitude-versus-offset variations in gas sands: Geophysics, 54**,** 680-688.

Smith, G.C., and Gidlow, P.M., 1987, Weighted stacking for rock property estimation and detection of gas: Geophysical Prospecting, 35, 993-1014.

Whitcombe, D., Connolly, P., and Redshaw, T., 2002, Extended elastic impedance for fluid and lithology prediction, Geophysics, 67, 63-67.

Wiggins, R., Kenny, G.S., and McClure, C.D., 1983, A method for determining and displaying the shear-velocity reflectivities of a geologic formation: European patent Application 0113944.